Reactivity and Evolution of Ionic Phases in the Lithium Solid–Electrolyte Interphase

Reactivity and Evolution of Ionic Phases in the Lithium Solid-Electrolyte-Interphase

*Rui Guo†, Dongniu Wang§, Lucia Zuin§ and Betar M. Gallant†**

†Department of Mechanical Engineering, Massachusetts Institute of Technology, Cambridge, MA 02139, United States

§Canadian Light Source Inc., 44 Innovation Boulevard, Saskatoon, Saskatchewan S7N 2V3, Canada

Corresponding Author

*bgallant@mit.edu

ABSTRACT

The unstable solid electrolyte interphase (SEI) on Li anodes is the origin of major performance challenges in Li batteries, namely insufficient Coulombic efficiency (CE) and cycle life. While it is known that the SEI participates in aging processes, pinpointing the chemical origins by tracing them to specific SEI phases has been experimentally challenging. Here, we formed single-phase, thin (<50 nm) interfaces of Li_2O or LiF — the two most-common ionic SEI phases — on Li, and investigated their stability upon immersion in ether- or carbonate-based electrolytes. Contrary to some conventional wisdom that ionic phases are stable, we find by electrochemical impedance and X-ray spectroscopy that ionic SEI|electrolyte interfaces can undergo significant chemical evolution. While DOL/DME electrolytes impart minimal changes, organic/F-rich layers evolve at interfaces between Li_2O or LiF and carbonate electrolyte containing $LiPF_6$ salt, exacerbating subsequent plating overpotentials. The results suggest electrolyte selection is important to improve transport in ionic-rich Li interfaces.

TOC GRAPHIC

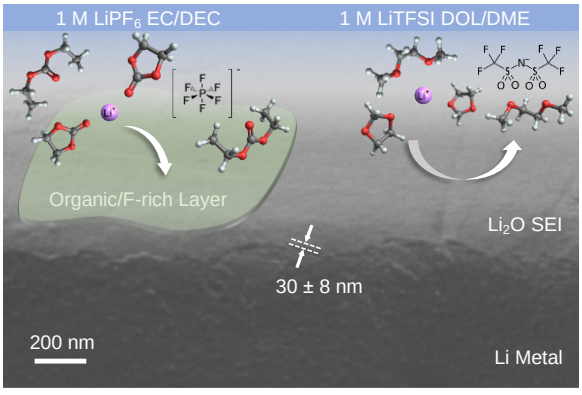

Recent years have seen a dramatic and renewed emphasis on enabling use of Li as the anode in next-generation rechargeable batteries due to its substantially higher capacity (3,860 mAh/g theoretical) than graphite (372 mAh/g theoretical).[1, 2] However, major challenges of low Coulombic efficiency (CE, ~99%, less than 99.9% or greater needed for electric vehicles) and insufficient cycle life persist. These challenges are traced to the nanoscale, electrolyte-derived, ionically-conductive solid electrolyte interphase (SEI) that forms as a result of thermodynamically-driven Li/electrolyte reactivity.[3] The fragile SEI is unstable to varying degrees in all known electrolytes as Li is plated or stripped, resulting in a less-than-unity CE.

In the classical models put forward by Peled and Aurbach involving mosaic and layered descriptions of the SEI, ionic phases, namely Li_2O and LiF, are enriched closest to the lithium interface in carbonate- or ether-based electrolytes.[4-8] These observations arise largely from experimental findings by X-ray photoelectron spectroscopy (XPS), where depth-profiling tends to show enhanced ionic species farther from the electrolyte and deeper into the buried interface.[5] The predominance of these ionic phases closest to Li has been rationalized by the fact that only the fully-reduced ionic phases are stable in contact with Li. Meanwhile, the outer portions of the SEI are highly electrolyte-dependent, and have generally been assigned to less-reduced species. For example, Li_2CO_3 and semi-carbonates are enriched in the outer SEI in carbonate-based electrolytes, [5, 9, 10] while more Li alkoxide and elastomers are formed in ether-based electrolytes, contributing to improved Coulombic efficiency of Li anode.[6-8] There is still an imprecise picture of how the mosaic or multi-layered structure of the SEI becomes established. For instance, descriptions of SEI growth invoke, at a high level, electron tunneling, typically confined to the first ~1 nm, from metallic Li to solvent and salt, followed by a slower growth of the SEI outer layer which has been attributed variably to dissolution/deposition reactions and/or “aging” of the

SEI, processes that are still not well-understood.[3] Meanwhile, the primary SEI-forming reactions are often described as resulting from direct reactivity between Li metal and electrolyte; less is known about the interplay between SEI phases and electrolyte once those phases become present within an SEI.

Oxygenated SEI phases such as LiOH and Li_2O were found early on by Aurbach to react, given their basicity, with γ-butyrolactone, forming hydroxy- or alkoxybutyrate, respectively[11]. Such reactivity was suggested to extend generally to other electrophilic solvent molecules such as carbonates.[6] Balbuena et al.[12, 13] more recently modeled thin (~1 nm), single-phase inorganic interfaces (Li_2O, LiOH, and Li_2CO_3) on Li metal in the presence of explicit solvent and salt molecules (LiTFSI or LiFSI in DME) by ab initio molecular dynamics (AIMD) calculations. Li_2O exhibited little chemical reactivity with DME molecules, although the solvent was found to lead to some Li dissolution due to solvation driving forces, resulting in off-stoichoimetry in Li_2O.[12] In contrast, chemical reactivity was observed between Li_2O and LiTFSI[12] and moreso with LiFSI, which fragmented into multiple smaller compounds.[13] There is still a lack of experimental studies on the stability and reactivity of individual phases within the SEI|electrolyte interface, making it challenging to validate these predictions and gage the extent and impact of such reactions. To guide future efforts at rational electrolyte-facing and interface modification strategies, many of which enrich the SEI with ionic phases like Li_2O and LiF,[14-18] improving understanding of SEI stability with specificity towards individual SEI phases and electrolyte formulations will be highly informative.

Here, we show that nominally 'stable' phases, Li_2O and LiF, are subject to continued reactivity with certain electrolytes, particularly those containing $LiPF_6$ salt and to a lesser extent, carbonate solvents. The reactivity is unambiguously found by several complementary spectroscopy

techniques including electrochemical impedance spectroscopy (EIS), X-ray photoelectron spectroscopy (XPS), and X-ray absorption near-edge spectroscopy (XANES). In particular, we find that Li_2O readily evolves to contain fluorine-rich ionic and organic phases in the outer-region of the SEI, even when the Li_2O is sufficiently thick (~30 nm) to block electron tunneling. The resulting chemical changes facing the electrolyte directly impact transport through the SEI as this is the site where Li^+ desolvate and transfer into the SEI, and can lead to problematically higher overpotentials required to drive Li plating.

Single-phase, conformal, polycrystalline Li_2O or LiF SEI on Li metal (Li|Li_2O or Li|LiF, respectively) were prepared by controlled reaction of rolled and polished Li foils with O_2 or with nitrogen trifluoride (NF_3) gas at 175°C for 1 hour, following an approach described in our previous publications[19, 20] which discuss the thickness, morphology, chemical composition and temperature dependence of the single-component interfaces SEI in detail. We begin by describing results on the Li_2O SEI. The average thickness of the as-prepared interface was measured to be 30 ± 8 nm by cross-sectional SEM imaging as shown in Fig. 1a, and the formed interfaces were qualitatively observed to be free of observable defects such as holes or cracks as indicated by top-view SEM images shown in Fig. S1. The composition was confirmed by Li K-edge fluorescence yield (FLY) XANES to be overwhelmingly Li_2O, as shown in Fig. 1b. As Li_2O is highly reactive towards trace CO_2 contamination present even to limited degree in the sample preparation and transfer processes for characterization, Li_2CO_3 was found to an extent on unsoaked (and thus unprotected) Li_2O SEI samples by both XPS and highly surface-sensitive Li K-edge total electron yield (TEY) XANES, as shown in Fig. S2. The obtained interfaces are advantageous for reactivity studies because the Li_2O thickness is sufficient to block direct Li-electrolyte contact and rule out electron tunneling from Li, thus isolating reactivity at the SEI-electrolyte interface, while providing sufficient

'enhancement' of Li_2O material (compared to a native interface of <10 nm) to allow for meaningful spectroscopic characterization. The chemically blocking nature of the Li_2O interface was confirmed by gas chromatography measurements upon soaking Li|Li_2O electrodes in carbonate electrolyte (Fig. S3), which showed distinct gas fingerprints compared to unprotected Li, indicating that the Li_2O inhibited direct Li-electrolyte reactivity and that the Li_2O SEI densely covers the Li surface. Similar observations of Li|LiF electrodes were reported in our previous publication.[20] In addition, the Li_2O films are polycrystalline and derived from Li metal, thus have microstructural features and chemical potential more similar to a native SEI than bulk Li_2O powders, even though Li_2O formed by metal-gas reaction may not be a perfect analogue of Li_2O in native SEI formed by electrochemical reactions. Note that the Li_2O is thin enough to enable Li^+ transport, although at the cost of higher overpotentials as will be discussed later.

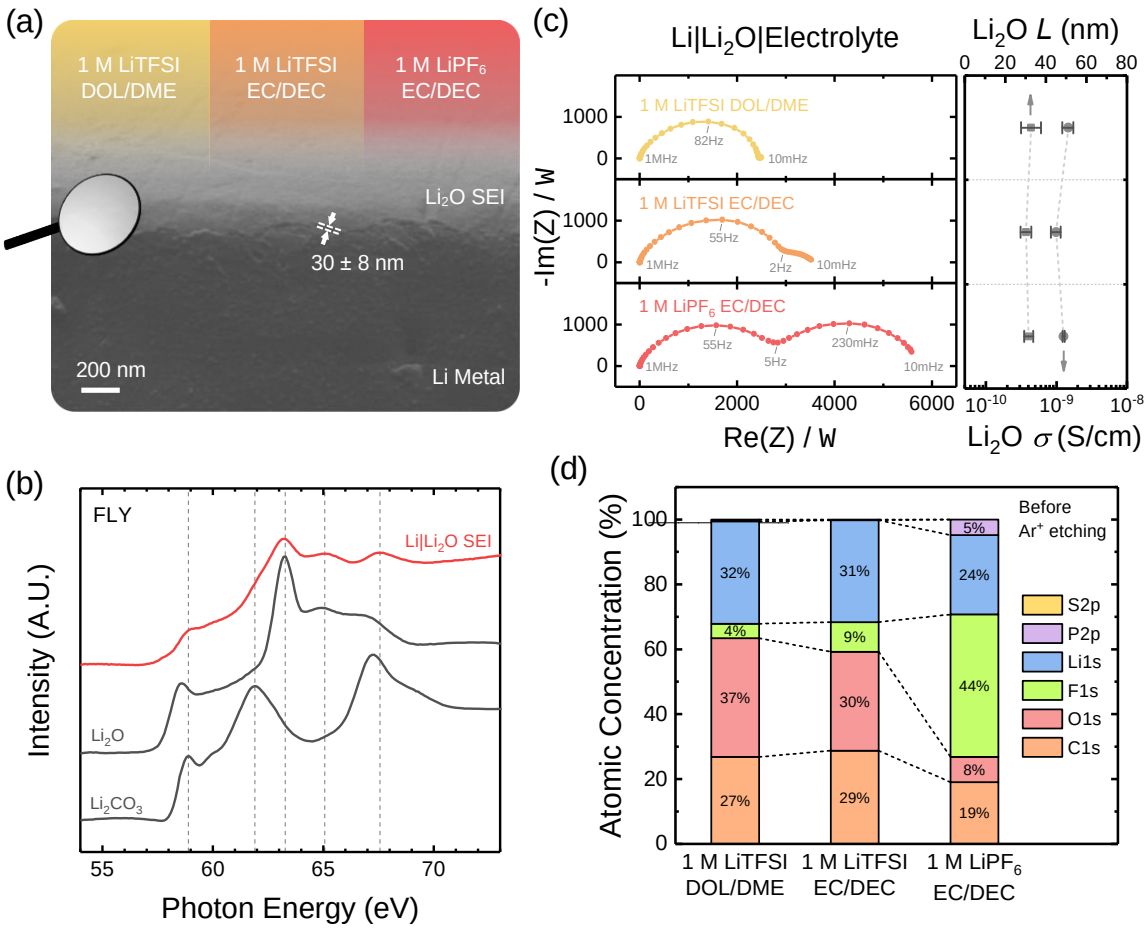

Figure 1. (a) Schematic of interactions probed between ether or carbonate-based electrolytes and the Li_2O SEI prepared on Li metal with a characteristic thickness of 30 ± 8 nm. (b) Li K-edge FLY XANES spectra of as-prepared Li|Li_2O SEI compared with standard powder samples of Li_2O and Li_2CO_3.[21] (c) EIS spectra of Li|Li_2O SEI in the three different electrolytes indicated in (a), where the thickness L and conductivity σ of the Li_2O SEI were acquired by fitting the higher-frequency semi-circle (or the sole semi-circle in the case of DOL/DME).[19] (d) Atomic concentrations obtained by XPS on the surface of Li|Li_2O SEI soaked in the three different electrolytes for 12 hours.

Three electrolytes were examined for each interface – two carbonate-based (1 M $LiPF_6$ EC/DEC, 1 M LiTFSI EC/DEC) and one ether-based (i.e., 1 M LiTFSI DOL/DME). To first examine the

chemical stability of the formed interfaces, EIS measurements of symmetric coin cells assembled with two Li|Li_2O electrodes and each of the above three electrolytes were conducted. Cells were assembled and rested for 6 hours prior to EIS measurements, which were found to yield stable spectra (Fig. S4). A non-reactive interface would be expected to yield an impedance result that is invariant with electrolyte, mainly reflecting the response of the ionically-resistive Li_2O. Counter to this picture, the EIS spectra of the Li_2O SEI exhibited distinct electrolyte-dependent features. As shown in Fig. 1c, a single semicircle ranging from 1 MHz to 10 mHz was observed in 1 M LiTFSI DOL/DME electrolyte. In contrast, an additional small, yet distinctive, lower-frequency semi-circle emerged ranging from 2 Hz to 10 mHz in 1 M LiTFSI EC/DEC electrolyte, while two distinct semicircles of similar size in both high- and low-frequency regions were observed in 1 M $LiPF_6$ EC/DEC ranging from 1 MHz to 5 Hz and 5 Hz to 10 mHz, respectively (Fig.1c). The lower-frequency semi-circle that emerged upon soaking in $LiPF_6$ EC/DEC was retained to a significant extent when EIS measurements were subsequently conducted in LiTFSI in DOL/DME (Fig. S5 and additional discussion). These differences, showing unique electrolyte-dependent features that are also distinct from the EIS spectra of pristine Li electrodes (Fig. S6), reflect strikingly different properties arising at the interface in spite of the fact that the nominal composition (Li_2O) is the same.

Previous studies showed that the high-frequency semicircle (typically 100 kHz to 20 Hz) is attributable to charge transfer through the most ionic and compact phases of the SEI, which here comprises the imparted Li_2O layer, i.e. the region closest to the Li interface.[22, 23] Meanwhile, the semicircle in the lower-frequency range represents an interface between Li_2O and electrolyte (the outer SEI).[24, 25] The real-valued magnitudes associated with the high-frequency semicircles were similar (2.7 ± 0.2 kΩ) across all samples, although the frequency associated with the semicircle

peak varied somewhat with the emergence of a lower-frequency feature, shifting to lower values (~55 Hz vs. 82 Hz) for carbonate vs. DOL/DME electrolyte, respectively. The clear frequency-separation of two impedance processes uniquely occurring in carbonate electrolytes suggests that a distinct chemical region emerges at the Li_2O-electrolyte interface. This also implies that the high-frequency region corresponds to the remaining unreacted Li_2O (compositional information as a function of near-surface vs. "bulk" SEI is presented later). Following our previous publication, we applied an equivalent circuit model originally developed by Churikov et al.[26, 27] to the high-frequency semi-circle in 1 M $LiPF_6$ EC/DEC and extracted select parameters of the pristine Li_2O portion of the SEI, namely the thickness of the ionic layer (shown previously to agree with independent thickness measurements by SEM and XPS depth-profiling) and ionic conductivity.[19] As shown in Fig. 1c, the unreacted Li_2O thickness found in the electrolyte-soaked samples herein was around 30 nm, similar to the as-prepared thickness within experimental error, indicating that any changes to the SEI resulted in growth rather than significant corrosion upon immersion of Li_2O in electrolyte. The conductivity attributed to the Li_2O portion of the EIS spectra was also similar across the three electrolytes at around 1.2×10^{-9} S/cm,[19] consistent with the fact that a substantial portion of Li_2O remained unreacted and physically and chemically distinct, with changes confined to the Li_2O|electrolyte interface. In addition to the gas evolution measurements which previously showed negligible direct Li-electrolyte reactivity upon soaking (Fig. S3), to further confirm that the EIS results accurately reflected the Li_2O interface, an experiment was conducted in which fresh Li was exposed by creating intentional cracks in the Li_2O layer prior to cell assembly. As shown in Fig. S7, the EIS measurements still predominantly reflect the response of the modified Li_2O interface even if there are certain amounts of minor cracks (< 5% of total surface area) whereas a large amount of cracks yields a markedly different response with

substantially lower impedance. The results collectively confirm that the EIS data reflect an intact Li|Li_2O|electrolyte interface (and not Li|electrolyte).

The atomic concentrations on the surface of the soaked Li_2O SEIs, as determined by XPS (Fig. 1d), also exhibited strong electrolyte-dependence. After immersion in 1 M LiTFSI DOL/DME, the Li_2O|electrolyte interface was rich in O and Li with only 4 at.% of F, indicating limited reactivity with the TFSI salt. In contrast, the F concentration increased to 9 at.% in 1 M LiTFSI EC/DEC and was even higher (44 at.%) in 1 M $LiPF_6$ EC/DEC. Thus, the F-rich Li_2O|electrolyte interface corresponds to the large low-frequency semicircle observed in the 1 M $LiPF_6$ EC/DEC electrolyte (Fig. 1c), suggesting that a F-rich Li_2O|electrolyte interface as the outer SEI layer results in an additional charge transfer barrier.

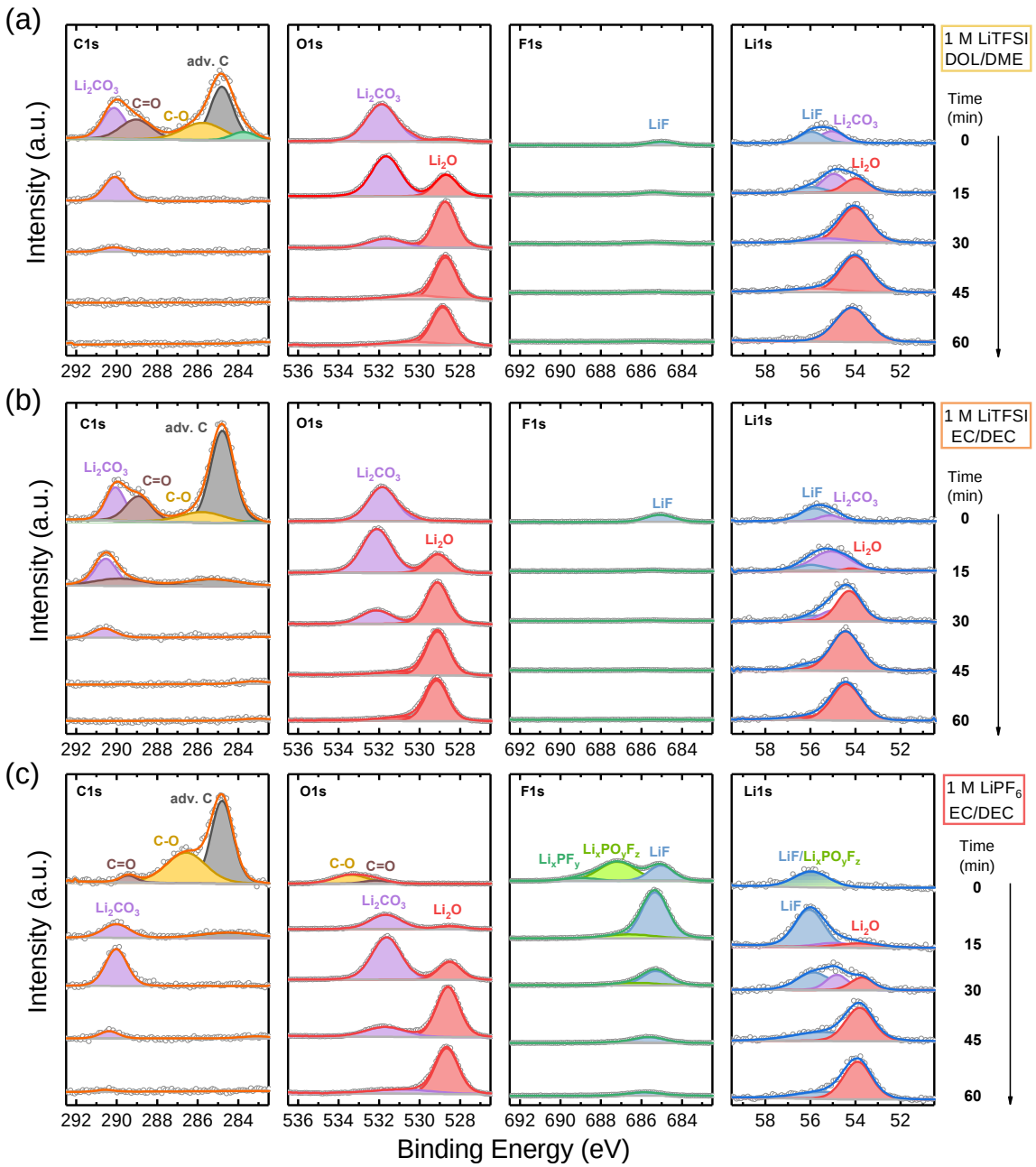

Figure 2. XPS depth profile of Li|Li_2O soaked in (a) 1 M LiTFSI DOL/DME, (b) 1 M LiTFSI EC/DEC and (c) 1 M $LiPF_6$ EC/DEC. The scaling factor of each element is the same in all panels (a-c). The Ar^+ etching rate was calibrated on an SiO_2 surface as approximately 1.4 nm/min.

To gain more insight into the nature of surface species, XPS depth profile was applied to further interrogate the chemical composition of the Li_2O|electrolyte interfaces, as shown in Fig. 2 (XPS

data on the native interface in each electrolyte are given in Fig. S8). When LiTFSI salt was used in either DOL/DME or EC/DEC solvent, the only F-containing species was found to be a very minor amount of LiF, indicated by the single F 1s peak at 685.0 eV, as shown in Fig. 2a and 2b. In contrast, significantly higher amounts of fluorinated species were observed in the $LiPF_6$-based EC/DEC electrolyte, and persisted deeper into the interface (Fig. 2c). Specifically, the presence of LiF at 685.0 eV, $Li_xPO_yF_z$ at 687.2 eV and Li_xPF_y at 688.9 eV indicate significant side reactions unique to the presence of the PF_6^- anion.[28-30] In addition, the organic species on the soaked Li_2O SEI surfaces were also found to be very different in the three electrolytes. With LiTFSI, the C 1s spectra in Fig. 2a and 2b were similar, albeit with higher C=O (288.9 eV) to C-O (285.8 eV) ratio in the carbonate electrolyte (1.4:1 in 1 M LiTFSI EC/DEC) than that in the ether electrolyte (0.87:1 in 1 M LiTFSI DOL/DME). However, in the case of 1 M $LiPF_6$ EC/DEC electrolyte, the Li_2O SEI surface was overwhelmingly dominated by the C-O bonding at 286.6 eV in C 1s and 533.4 eV in O 1s, which could be related to the decomposed carbonate solvent forming species such as poly(ethylene oxide) (PEO) on the Li_2O|electrolyte interface.[28, 31-33] We term this newly formed layer as "organic/F-rich", since it also contained large amounts of LiF and other fluorinated species. We note that Li_2CO_3 was observed on the top surface of Li_2O soaked in the TFSI-based electrolytes (DOL/DME and EC/DEC) as indicated by peaks at 531.5 eV in O 1s, 289.8 eV in C 1s and 55.0 eV in Li 1s.[34] We attribute this to the lesser degree of reactivity between Li_2O and these electrolytes, leaving more unreacted Li_2O which became subject to reaction with trace CO_2 contaminants as described previously. We also note in Fig. 2 that only pure Li_2O was observed after prolonged etching following removal of organic or F-containing species, indicating that electrolytes did not completely penetrate the Li_2O SEI and react with Li metal directly, which is consistent with our other findings (Fig. S3, S7). Unfortunately, while commonly relied-upon, XPS

Ar^+ etching is highly destructive and can introduce chemical artefacts into the sample, particularly as carbon, oxygenates and carbonates are aggressively generated in the gas-phase nearby the highly-reactive pristine Li_2O; for instance, continued sputtering revealed re-formation of Li_2CO_3 in all electrolytes at various depths into the interface in spite of the fact that Li_2O was the predominant phase indicated by XANES in the bulk (Fig. 1c).

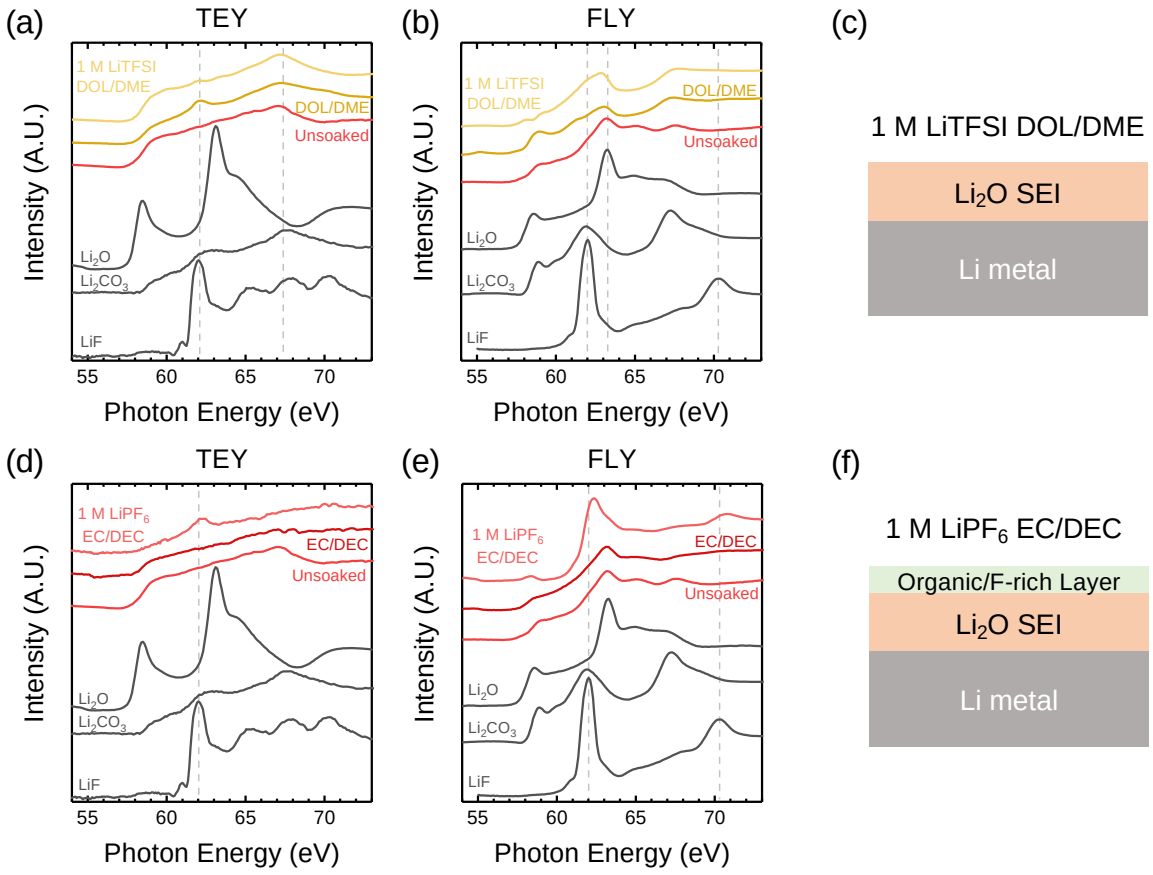

Figure 3. (a) TEY and (b) FLY Li K-edge XANES of the Li|Li_2O interface after being soaked in DOL/DME solvent or 1 M LiTFSI DOL/DME electrolyte for 20 hours. (c) A schematic showing the resulting Li|Li_2O interface in 1 M LiTFSI DOL/DME electrolyte. (d) TEY and (e) FLY of Li K-edge XANES of Li|Li_2O interface after being soaked in EC/DEC solvent or 1 M $LiPF_6$ EC/DEC electrolyte for 20 hours. (f) A schematic showing the resulting Li|Li_2O interface in 1 M $LiPF_6$ EC/DEC electrolyte.

Thus, to more carefully examine the extent of electrolyte reactivity in the Li_2O interface, we further applied non-destructive Li K-edge XANES for interface analysis. TEY is highly surface sensitive with a probing length of less than 5 nm at Li K-edge, however, FLY is more bulk sensitive with an X-ray attenuation length between 40 and 60 nm across the Li K-edge, which indicate that photons can ideally probe the entire SEI interfacial layer with a thickness of ~30 nm.[21] This is confirmed by a weak Li metal adsorption edge at ~55 eV observed in the as-prepared Li|Li_2O SEI (Fig. S9). The Li K-edge TEY (Fig. 3a) of Li_2O SEI soaked in 1 M LiTFSI in DOL/DME electrolyte only indicated minor differences from the unsoaked sample in surface Li_2CO_3 contamination at 62.0 eV and 67.2 eV, while the FLY (Fig. 3b) showed insignificant changes compared with the unsoaked sample, further supporting that the 1 M LiTFSI DOL/DME electrolyte has a limited effect on altering the chemical composition of Li|Li_2O SEI, as summarized in Fig. 3c. However, when the Li_2O SEI was exposed to 1 M $LiPF_6$ EC/DEC electrolyte, a dominant LiF peak emerged at 62.3 eV in both the TEY (Fig. 3d) and FLY (Fig. 3e) of Li K-edge XANES, with a slight blue shift towards higher energy level compared with the standard LiF peak at 62.0 eV. Wang and Zuin[21] reported a similar Li K-edge blue shift in wet $LiPF_6$ salt with EC/DEC solvent, where the ionic bonding of $LiPF_6$ could be strengthened by salt-solvent interactions. Therefore, the blue shift of the LiF peak (62.3 eV) observed in Fig. 3e may also be attributed to solvation of ionic phases within an organic-rich phase of the reacted SEI. The LiF signal in TEY (Fig. 3d) was also much more suppressed than FLY (Fig. 3e), possibly due to the presence of an amorphous organic-rich surface layer as schematized in Fig. 3f.

These results collectively indicate that the reactivity of Li_2O with LiTFSI salt is relatively minor. The more severe interfacial reactions occur with carbonate solvent present and particularly in the presence of $LiPF_6$, leading the Li_2O interface to involve into more stable fluorinated phases. $LiPF_6$

salt is well-known to undergo decomposition reactions in the presence of water and thus possible formation mechanisms of the organic/F-rich layer on Li_2O SEI can be proposed:[35, 36]

$LiPF_6 \rightarrow PF_5 + LiF$ (1)

$PF_5 + H_2O \rightarrow POF_3 + HF$ (2)

$POF_3 + Li_2O \rightarrow Li_xPO_yF_z + LiF$ (3)

$Li_2O + 2HF \rightarrow H_2O + 2LiF$ (4)

$(CH_2O)_2CO \xrightarrow{PF_5} (\text{-}CH_2\text{-}CH_2\text{-}O\text{-}) + CO_2$ (5)

We note that Li_2CO_3 surface contamination could also exhibit reactivity towards $LiPF_6$ electrolyte (e.g., $LiPF_6 + Li_2CO_3 \rightarrow 3LiF + POF_3 + CO_2$) and cannot be ruled out as a possible contribution to the observed interfacial changes.[36]

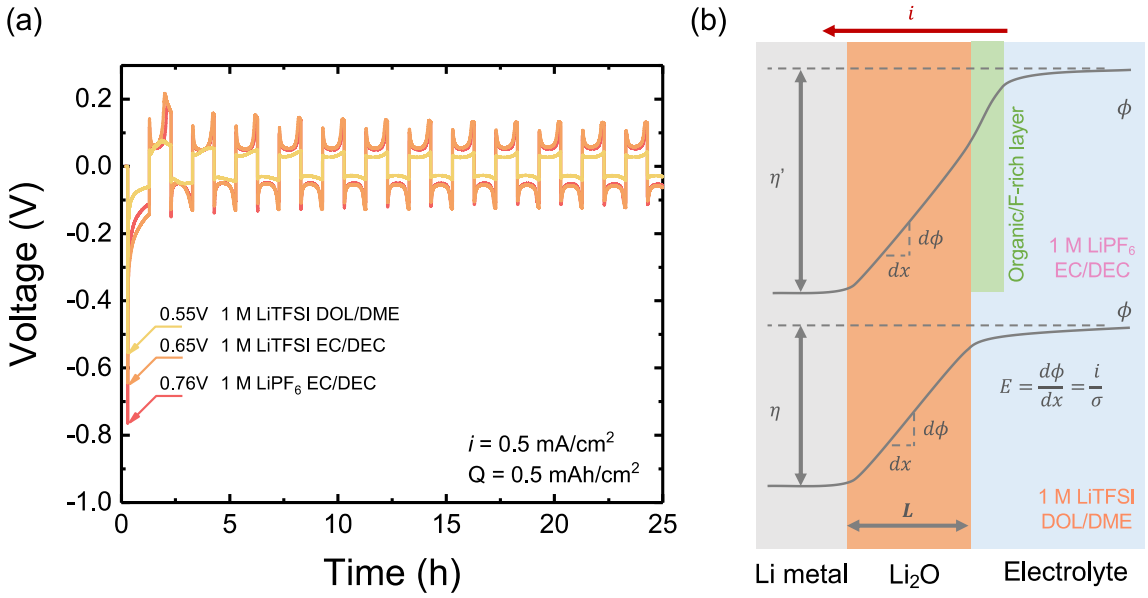

Figure 4. (a) Cycling performance of Li|Li_2O electrodes in a symmetric coin cell with different electrolytes. (b) A schematic showing the potential gradient and overpotential across the Li SEI.

The chemical nature of the Li_2O|electrolyte interface, as revealed by XPS and Li K-edge XANES measurements is significant because it relates to its transport through the interface, and could result in comparable or even larger charge transfer barrier than the bulk SEI layer if not carefully

designed. We investigated the influence of the different Li_2O|electrolyte interfaces on the electrochemical cycling of the Li electrode in symmetric Li|Li_2O cells at a current density of 0.5 mA/cm^2, as shown in Fig. 4a. High initial overpotentials on the first stripping/plating cycle were found in all three electrolytes, varying from 0.55 V in 1 M LiTFSI DOL/DME to 0.65 V in 1 M LiTFSI EC/DEC, and 0.76 V in 1 M $LiPF_6$ EC/DEC. The trends in overpotential agree qualitatively with the increasing degree of interfacial reactivity towards fluorinated species. As shown in a schematic in Fig. 4b, the enhanced resistance due to the organic/F-rich layer will require larger initial overpotential to meet the current demanded in the cell, which can create large electric fields across the SEI and invite potential breakdown. For example, theoretically, perfect ion conduction through an intact Li_2O SEI, assuming an ionic conductivity of $\sigma = 1.2 \times 10^{-9}$ S/cm and current density 0.5 mA/cm^2, predicts an electric field as high as $E = i/\sigma \approx 42$ MV/m across the Li_2O. This value is significantly higher than the dielectric strengths of common metal oxides (Al_2O_3, BeO and ZrO_2) of approximately 11–13 MV/m.[37] We hypothesize that such a breakdown process could be responsible for the initially higher plating overpotential, which is not repeated on subsequent cycles. The magnitude of the fields experienced in these *ex situ* SEI may be larger than those in a typical native SEI due to the fact that these Li_2O interfaces, though of comparable thickness to a native SEI, are entirely ionic and thus potentially possess higher total resistance. However, we note that initially large plating overpotentials are commonly observed across a wide range of electrolytes and are not unique to the Li_2O interfaces studied herein.[38, 39] Following this initially high overpotential, we observed an immediate drop of overpotentials during the first discharge step in all three electrolytes, and lower cycling overpotentials closer to that of pristine Li cycling (Fig. S10) were sustained thereafter, suggesting that fresh Li deposits contacted the

electrolyte and formed native SEI after the initial cycle. This could be confirmed by SEM images after an initial plating step (Fig. S11).

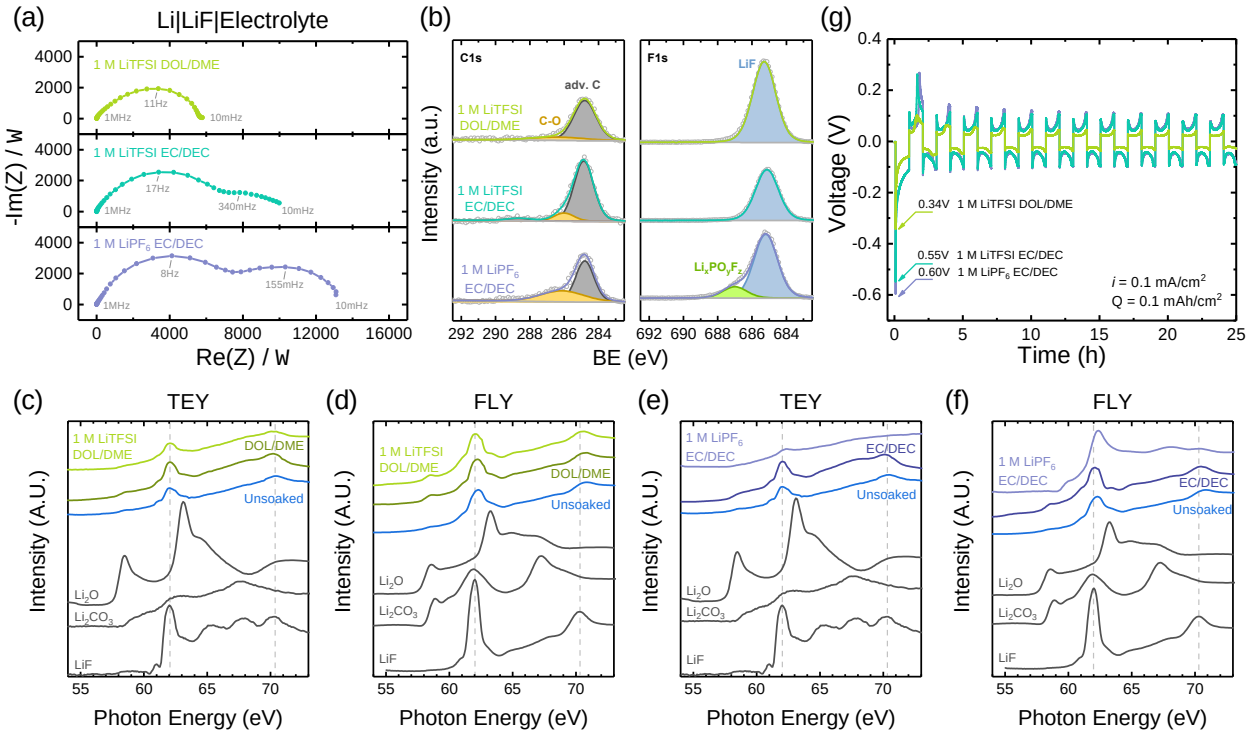

Figure 5. (a) EIS spectra of Li|LiF SEI in the 3 different electrolytes. (b) C1s and F1s XPS of the surface layer of Li|LiF SEI after being soaked in electrolytes. (c) TEY and (d) FLY of Li K-edge XANES of Li|LiF interface after being soaked in DOL/DME solvent or 1 M LiTFSI DOL/DME electrolyte for 20 hours. (e) TEY and (f) FLY of Li K-edge XANES of Li|LiF interface after being soaked in EC/DEC solvent or 1 M $LiPF_6$ EC/DEC electrolyte and for 20 hours. (g) Cycling performance of Li|LiF electrodes in a symmetric coin cell with different electrolytes.

We next investigated the interface between LiF and the same electrolytes, since LiF has been regarded as an important species enabling a more stable SEI, due to its wide electrochemical stability window, high shear modulus and low electronic conductivity.[15, 40, 41] Herein, the Li|LiF SEI was also prepared by metal-gas reaction using NF_3 gas, as discussed in our previous publication.[20] The unsoaked LiF SEI showed an enhanced shoulder in both XANES FLY and TEY

above the standard LiF peak at 62.0 eV, indicating possible structural distortion of the LiF SEI grown on the surface of Li metal. Unexpectedly, the EIS results of LiF SEI in different electrolytes (Fig. 5a) showed that the LiF|electrolyte interface also experienced electrolyte-dependent changes that were qualitatively similar to Li_2O. In 1 M LiTFSI DOL/DME, negligible reactivity was observed as indicated by the retention of a single high-frequency semi-circle, while the carbonate-based electrolytes (1 M LiTFSI EC/DEC and 1 M $LiPF_6$ EC/DEC) induced more significant changes as indicated by the emergence of lower-frequency semi-circles that were most severe with $LiPF_6$. $LiPF_6$ salt in particular led to an increase in surface organic species as indicated by C-O bonding (286.6 eV) and decomposition products of $Li_xPO_yF_z$ (687.2 eV) as determined from XPS (Fig. 5b and Fig. S12), indicating a more complex LiF|electrolyte interface. Both TEY (Fig. 5c) and FLY (Fig. 5d) XANES supported that LiF changed little in 1 M LiTFSI DOL/DME. However, after the LiF SEI was soaked in 1 M $LiPF_6$ EC/DEC, the TEY spectra showed an attenuated LiF signal, possibly due to increased amounts of organic species on the surface (Fig. 5e); meanwhile FLY spectra (Fig. 5f) displayed an enhanced LiF peak with a blue shift similar to the case of the Li_2O SEI (Fig. 3e), indicating strong interactions between surface fluorinated species and organic solvents. These changes were again reflected in cycling data in symmetric Li|LiF cells, which revealed a smaller overpotential for 1 M LiTFSI DOL/DME (0.34 V), followed by increasing overpotentials for 1 M LiTFSI in EC/DEC (0.55 V) and 1 M $LiPF_6$ in EC/DEC (0.60 V). Note that the higher resistance of LiF ($\sigma \approx 5.2 \times 10^{-10}$ S/cm)[19] necessitated even lower cycling currents (0.1 mA/cm^2) and also lower capacities (0.1 mAh/cm^2) compared to Li_2O.

Although LiF is less nucleophilic than Li_2O and is not conventionally considered to be reactive, some computational studies have suggested otherwise. In addition to salt reactivity with Li_2O discussed previously, Balbuena et al.[13] observed reduction of $TFSI^-$ and FSI^- anions on the surface

of an LiF layer by AIMD simulations. Our results suggest this to be a relatively minor although not insignificant source of interfacial compositional changes. In addition, the LiF surface has been confirmed by adsorption calorimetry to be capable of adsorbing polar molecules such as H_2O (μ=1.84 D) and CH_3OH (μ=1.59 D).[42] EC has a much higher dipole moment (μ_{EC}=4.61 D) than most ethers (e.g., μ_{DME}=1.71 D and μ_{DOL}=1.19 D), therefore the additional transport barrier observed in EC/DEC electrolyte compared to DOL/DME could potentially arise from surface adsorption of EC molecules on the LiF surface, which may also invite subsequent reactions. Okuno et al.[43] calculated the interface structure between LiF and dilithium ethylene dicarbonate (Li_2EDC) aggregates via DFT-MD, and found strong adsorption of Li_2EDC – one of EC decomposition products[33] – on the LiF surface. These studies collectively make it plausible that decomposition products of EC in particular, induced by HF and PF_5 reactivity in $LiPF_6$-containing electrolytes, can become strongly adsorbed on the surface of LiF SEI.

Our results shed light on the fact that ionic phases in the SEI, particularly in certain electrolytes, can undergo dynamic evolution that significantly influences transport through the interface in ways that decrease the SEI stability. This reactivity is particularly exacerbated in carbonate-based electrolytes, especially when reactive salts such as $LiPF_6$ are used. Although continued studies of SEI chemical reactivity are needed, the results provide one set of data to help rationalize the conventional mosaic picture of the SEI that describe the co-existence of multiple ionic phases, however revealing a new twist: certain ionic phases (e.g. Li_2O) can actually beget other ionic phases (e.g. LiF), such that direct reactivity between Li metal and fluorinated electrolyte constituents need not be the only source of fluorinated species in the interface. It is important to note that, in addition to Li_2O and LiF, other ionic phases may also coexist in the SEI (e.g., Li_2CO_3, Li_xC and Li_3N), and contribute to the properties and performance of Li SEI.[44] We recall that recent

cryo-EM studies, along with some earlier studies, have revealed unexpected nanocrystalline ionic phases such as Li_2O[16, 17, 45] or LiF[18, 46] in the outer electrolyte-facing portion of the SEI in some electrolytes, indicating a potential source of continued reactivity that should be considered in rational design of improved native SEI. Specifically, the chemical insights obtained herein suggest that in electrolytes that favor Li_2O formation, it may be desirable to avoid use of Li_2O-reactive fluorinated salts to keep ionic resistance to a minimum and support lower plating overpotentials. In addition, these findings may have direct implications for *ex situ* modification approaches for Li: it is critical to examine the reactivity of such interfaces with the electrolyte to ensure that modified interfaces are truly protective and stable.

ASSOCIATED CONTENT

Supporting Information. Experimental materials and methods; SEM images of Li_2O SEI; Nyquist plot of EIS data; and XANES spectra of Li_2O SEI (PDF)

AUTHOR INFORMATION

Corresponding Author

Betar M. Gallant – Department of Mechanical Engineering, Massachusetts Institute of Technology, Cambridge, MA 02139, United States; Email: bgallant@mit.edu

Authors

Rui Guo – Department of Mechanical Engineering, Massachusetts Institute of Technology, Cambridge, MA 02139, United States

Dongniu Wang – Canadian Light Source Inc., 44 Innovation Boulevard, Saskatoon, Saskatchewan S7N 2V3, Canada

Lucia Zuin – Canadian Light Source Inc., 44 Innovation Boulevard, Saskatoon, Saskatchewan S7N 2V3, Canada

Notes

The authors declare no competing financial interest.

ACKNOWLEDGMENT

The authors gratefully acknowledge support from the National Science Foundation under award number 1804247. This work made use of the MRSEC Shared Experimental Facilities at MIT, supported by the National Science Foundation under award number DMR-1419807. XANES data described in this paper were collected at the VLS-PGM beamline in Canadian Light Source, a national research facility of the University of Saskatchewan, which is supported by the Canada Foundation for Innovation (CFI), the Natural Sciences and Engineering Research Council (NSERC), the National Research Council (NRC), the Canadian Institutes of Health Research (CIHR), the Government of Saskatchewan, and the University of Saskatchewan. The authors also thank Gustavo M. Hobold for helping with the gas chromatography measurements.

REFERENCES

1. Lin, D. C.; Liu, Y. Y.; Cui, Y., Reviving the Lithium Metal Anode for High-Energy Batteries. *Nat. Nanotechnol.* **2017,** *12* (3), 194-206.

2. Liu, J.; Bao, Z.; Cui, Y.; Dufek, E. J.; Goodenough, J. B.; Khalifah, P.; Li, Q.; Liaw, B. Y.; Liu, P.; Manthiram, A.; Meng, Y. S.; Subramanian, V. R.; Toney, M. F.; Viswanathan,

V. V.; Whittingham, M. S.; Xiao, J.; Xu, W.; Yang, J.; Yang, X.-Q.; Zhang, J.-G., Pathways for Practical High-Energy Long-Cycling Lithium Metal Batteries. *Nat. Energy* **2019,** *4* (3), 180-186.

3. Peled, E.; Menkin, S., Review-SEI: Past, Present and Future. *J. Electrochem. Soc.* **2017,** *164* (7), A1703-A1719.

4. Peled, E.; Golodnitsky, D.; Ardel, G., Advanced Model for Solid Electrolyte Interphase Electrodes in Liquid and Polymer Electrolytes. *J. Electrochem. Soc.* **1997,** *144* (8), L208-L210.

5. Schechter, A.; Aurbach, D.; Cohen , H., X-Ray Photoelectron Spectroscopy Study of Surface Films Formed on Li Electrodes Freshly Prepared in Alkyl Carbonate Solutions. *Langmuir* **1999,** *15* (9), 3334-3342.

6. Aurbach, D., Review of Selected Electrode-Solution Interactions Which Determine the Performance of Li and Li Ion Batteries. *J. Power Sources* **2000,** *89* (2), 206-218.

7. Gofer, Y.; Benzion, M.; Aurbach, D., Solutions of $LiAsF_6$ in 1,3-Dioxolane for Secondary Lithium Batteries. *J. Power Sources* **1992,** *39* (2), 163-178.

8. Aurbach, D.; Daroux, M. L.; Faguy, P. W.; Yeager, E., Identification of Surface-Films Formed on Lithium in Dimethoxyethane and Tetrahydrofuran Solutions. *J. Electrochem. Soc.* **1988,** *135* (8), 1863-1871.

9. Aurbach, D.; Einely, Y.; Zaban, A., The Surface-Chemistry of Lithium Electrodes in Alkyl Carbonate Solutions. *J. Electrochem. Soc.* **1994,** *141* (1), L1-L3.

10. Aurbach, D.; Markovsky, B.; Shechter, A.; EinEli, Y.; Cohen, H., A Comparative Study of Synthetic Graphite and Li Electrodes in Electrolyte Solutions Based on Ethylene Carbonate Dimethyl Carbonate Mixtures. *J. Electrochem. Soc.* **1996,** *143* (12), 3809-3820.

11. Aurbach, D., Identification of Surface Films Formed on Lithium Surfaces in Γ-Butyrolactone Solutions: II. Contaminated Solutions. *J. Electrochem. Soc.* **1989,** *136* (6), 1611.

12. Kamphaus, E. P.; Angarita-Gomez, S.; Qin, X. P.; Shao, M. H.; Engelhard, M.; Mueller, K. T.; Murugesan, V.; Balbuena, P. B., Role of Inorganic Surface Layer on Solid Electrolyte Interphase Evolution at Li-Metal Anodes. *ACS Appl. Mater. Interfaces* **2019,** *11* (34), 31467-31476.

13. Kamphaus, E. P.; Gomez, S. A.; Qin, X.; Shao, M.; Balbuena, P. B., Effects of Solid Electrolyte Interphase Components on the Reduction of LiFSI over Lithium Metal. *ChemPhysChem* **2020,** *21* (12), 1310-1317.

14. Lu, Y. Y.; Tu, Z. Y.; Archer, L. A., Stable Lithium Electrodeposition in Liquid and Nanoporous Solid Electrolytes. *Nat. Mater.* **2014,** *13* (10), 961-969.

15. Lin, D. C.; Liu, Y. Y.; Chen, W.; Zhou, G. M.; Liu, K.; Dunn, B.; Cui, Y., Conformal Lithium Fluoride Protection Layer on Three-Dimensional Lithium by Nonhazardous Gaseous Reagent Freon. *Nano Lett.* **2017,** *17* (6), 3731-3737.

16. Li, Y. Z.; Li, Y. B.; Pei, A. L.; Yan, K.; Sun, Y. M.; Wu, C. L.; Joubert, L. M.; Chin, R.; Koh, A. L.; Yu, Y.; Perrino, J.; Butz, B.; Chu, S.; Cui, Y., Atomic Structure of Sensitive Battery Materials and Interfaces Revealed by Cryo-Electron Microscopy. *Science* **2017,** *358* (6362), 506-510.

17. Li, Y. Z.; Huang, W.; Li, Y. B.; Pei, A.; Boyle, D. T.; Cui, Y., Correlating Structure and Function of Battery Interphases at Atomic Resolution Using Cryoelectron Microscopy. *Joule* **2018,** *2* (10), 2167-2177.

18. Huang, W.; Wang, H.; Boyle, D. T.; Li, Y. Z.; Cui, Y., Resolving Nanoscopic and Mesoscopic Heterogeneity of Fluorinated Species in Battery Solid-Electrolyte Interphases by Cryogenic Electron Microscopy. *ACS Energy Lett.* **2020,** *5* (4), 1128-1135.

19. Guo, R.; Gallant, B. M., Li_2O Solid Electrolyte Interphase: Probing Transport Properties at the Chemical Potential of Lithium. *Chem. Mater.* **2020,** *32* (13), 5525-5533.

20. He, M.; Guo, R.; Hobold, G. M.; Gao, H.; Gallant, B. M., The Intrinsic Behavior of Lithium Fluoride in Solid Electrolyte Interphases on Lithium. *Proc. Natl. Acad. Sci. U.S.A.* **2020,** *117* (1), 73-79.

21. Wang, D.; Zuin, L., Li K-Edge X-Ray Absorption near Edge Structure Spectra for a Library of Lithium Compounds Applied in Lithium Batteries. *J. Power Sources* **2017,** *337*, 100-109.

22. Thevenin, J., Passivating Films on Lithium Electrodes - an Approach by Means of Electrode Impedance Spectroscopy. *J. Power Sources* **1985,** *14* (1-3), 45-52.

23. Aurbach, D.; Zaban, A.; Gofer, Y.; Abramson, O.; Benzion, M., Studies of Li Anodes in the Electrolyte System 2Me-THF/THF/Me-Furan/$LiAsF_6$. *J. Electrochem. Soc.* **1995,** *142* (3), 687-696.

24. Moshtev, R.; Puresheva, B., AC Impedance Study of the Lithum Electrode in Propylene Carbonate Solutions: Part I. Effect of the Surface Preparation on the Initial Impedance Parameters. *J. Electroanal. Chem.* **1984,** *180* (1-2), 609-617.

25. Zaban, A.; Zinigrad, E.; Aurbach, D., Impedance Spectroscopy of Li Electrodes. 4. A General Simple Model of the Li-Solution Interphase in Polar Aprotic Systems. *J. Phys. Chem.* **1996,** *100* (8), 3089-3101.

26. Churikov, A. V.; Nimon, E. S.; Lvov, A. L., Impedance of Li-Sn, Li-Cd and Li-Sn-Cd Alloys in Propylene Carbonate Solution. *Electrochim. Acta* **1997,** *42* (2), 179-189.

27. Churikov, A. V.; Gamayunova, I. M.; Shirokov, A. V., Ionic Processes in Solid-Electrolyte Passivating Films on Lithium. *J. Solid State Electrochem.* **2000,** *4* (4), 216-224.

28. Markevich, E.; Salitra, G.; Aurbach, D., Fluoroethylene Carbonate as an Important Component for the Formation of an Effective Solid Electrolyte Interphase on Anodes and Cathodes for Advanced Li-Ion Batteries. *ACS Energy Lett.* **2017,** *2* (6), 1337-1345.

29. Nie, M. Y.; Abraham, D. P.; Chen, Y. J.; Bose, A.; Lucht, B. L., Silicon Solid Electrolyte Interphase (SEI) of Lithium Ion Battery Characterized by Microscopy and Spectroscopy. *J. Phys. Chem. C* **2013,** *117* (26), 13403-13412.

30. Baggetto, L.; Mohanty, D.; Meisner, R. A.; Bridges, C. A.; Daniel, C.; Wood, D. L.; Dudney, N. J.; Veith, G. M., Degradation Mechanisms of Lithium-Rich Nickel Manganese Cobalt Oxide Cathode Thin Films. *RSC Adv.* **2014,** *4* (45), 23364-23371.

31. Lux, S. F.; Chevalier, J.; Lucas, I. T.; Kostecki, R., HF Formation in $LiPF_6$-Based Organic Carbonate Electrolytes. *ECS Electrochem. Lett.* **2013,** *2* (12), A121-A123.

32. Jin, Y.; Kneusels, N. H.; Magusin, P.; Kim, G.; Castillo-Martinez, E.; Marbella, L. E.; Kerber, R. N.; Howe, D. J.; Paul, S.; Liu, T.; Grey, C. P., Identifying the Structural Basis for the

Increased Stability of the Solid Electrolyte Interphase Formed on Silicon with the Additive Fluoroethylene Carbonate. *J. Am. Chem. Soc.* **2017,** *139* (42), 14992-15004.

33. Michan, A. L.; Leskes, M.; Grey, C. P., Voltage Dependent Solid Electrolyte Interphase Formation in Silicon Electrodes: Monitoring the Formation of Organic Decomposition Products. *Chem. Mater.* **2015,** *28* (1), 385-398.

34. Wood, K. N.; Teeter, G., Xps on Li-Battery-Related Compounds: Analysis of Inorganic SEI Phases and a Methodology for Charge Correction. *ACS Appl. Energy Mater.* **2018,** *1* (9), 4493-4504.

35. Edström, K.; Gustafsson, T.; Thomas, J. O., The Cathode–Electrolyte Interface in the Li-Ion Battery. *Electrochim. Acta* **2004,** *50* (2), 397-403.

36. Eshetu, G. G.; Diemant, T.; Grugeon, S.; Behm, R. J.; Laruelle, S.; Armand, M.; Passerini, S., In-Depth Interfacial Chemistry and Reactivity Focused Investigation of Lithium–Imide- and Lithium–Imidazole-Based Electrolytes. *ACS Appl. Mater. Interfaces* **2016,** *8* (25), 16087-16100.

37. Berger, L., Dielectric Strength of Insulating Materials. *Carbon* **2006,** *1* (2006), 2.

38. Wood, K. N.; Kazyak, E.; Chadwick, A. F.; Chen, K. H.; Zhang, J. G.; Thornton, K.; Dasgupta, N. P., Dendrites and Pits: Untangling the Complex Behavior of Lithium Metal Anodes through Operando Video Microscopy. *ACS Cent. Sci.* **2016,** *2* (11), 790-801.

39. Bieker, G.; Winter, M.; Bieker, P., Electrochemical In Situ Investigations of SEI and Dendrite Formation on the Lithium Metal Anode. *Phys. Chem. Chem. Phys.* **2015,** *17* (14), 8670-8679.

40. Chen, L.; Chen, K. S.; Chen, X. J.; Ramirez, G.; Huang, Z. N.; Geise, N. R.; Steinruck, H. G.; Fisher, B. L.; Shahbazian-Yassar, R.; Toney, M. F.; Hersam, M. C.; Elam, J. W., Novel ALD Chemistry Enabled Low-Temperature Synthesis of Lithium Fluoride Coatings for Durable Lithium Anodes. *ACS Appl. Mater. Interfaces* **2018,** *10* (32), 26972-26981.

41. Zhao, J.; Liao, L.; Shi, F. F.; Lei, T.; Chen, G. X.; Pei, A.; Sun, J.; Yan, K.; Zhou, G. M.; Xie, J.; Liu, C.; Li, Y. Z.; Liang, Z.; Bao, Z. N.; Cui, Y., Surface Fluorination of Reactive Battery Anode Materials for Enhanced Stability. *J. Am. Chem. Soc.* **2017,** *139* (33), 11550-11558.

42. Yao, Y.-F. Y., Adsorption of Polar Molecules on Alkali-Fluorides. *J. Colloid Interface Sci.* **1968,** *28* (3-4), 376-385.

43. Okuno, Y.; Ushirogata, K.; Sodeyama, K.; Tateyama, Y., Decomposition of the Fluoroethylene Carbonate Additive and the Glue Effect of Lithium Fluoride Products for the Solid Electrolyte Interphase: An Ab Initio Study. *Phys. Chem. Chem. Phys.* **2016,** *18* (12), 8643-53.

44. Shi, S. Q.; Lu, P.; Liu, Z. Y.; Qi, Y.; Hector, L. G.; Li, H.; Harris, S. J., Direct Calculation of Li-Ion Transport in the Solid Electrolyte Interphase. *J. Am. Chem. Soc.* **2012,** *134* (37), 15476-15487.

45. Xu, Y.; Wu, H.; He, Y.; Chen, Q.; Zhang, J.-G.; Xu, W.; Wang, C., Atomic to Nanoscale Origin of Vinylene Carbonate Enhanced Cycling Stability of Lithium Metal Anode Revealed by Cryo-Transmission Electron Microscopy. *Nano Lett.* **2019,** *20* (1), 418-425.

46. Jurng, S.; Brown, Z. L.; Kim, J.; Lucht, B. L., Effect of Electrolyte on the Nanostructure of the Solid Electrolyte Interphase (SEI) and Performance of Lithium Metal Anodes. *Energy Environ. Sci.* **2018,** *11* (9), 2600-2608.